Correspondence

Iterative Detection of Unity-Rate Precoded FFH-MFSK and Irregular Variable-Length Coding

Sohail Ahmed, Robert G. Maunder, Lie-Liang Yang, and Lajos Hanzo

Abstract—Iterative decoding of an irregular variable-length coding (IrVLC) scheme concatenated with precoded fast frequency-hopping (FFH) M-ary frequency-shift keying (MFSK) is considered. We employ EXtrinsic Information Transfer (EXIT) charts to investigate the three-stage concatenation of the FFH-MFSK demodulator, the rate-1 decoder, and the outer IrVLC decoder. The proposed joint source and channel coding scheme is capable of operating at low signal-to-noise ratios (SNRs) in Rayleigh fading channels contaminated by partial-band noise jamming (PBNJ). The IrVLC scheme is composed of a number of component variable-length coding (VLC) codebooks employing different coding rates that encode particular fractions of the input source symbol stream. These fractions may be chosen with the aid of EXIT charts to shape the inverted EXIT curve of the IrVLC codec so that it can be matched with the EXIT curve of the inner decoder. We demonstrate that using the proposed scheme, an infinitesimally low bit error ratio (BER) may be achieved at low SNR values.

Index Terms—FEC, irregular channel coding, iterative detection of fast frequency-hopping (FFH) M-ary frequency-shift keying (MFSK), turbo-detection, unity-rate coding, variable-length coding (VLC).

I. INTRODUCTION

Fast frequency-hopping (FFH) M-ary frequency-shift keying (MFSK) has been shown to efficiently combat partial-band noise jamming (PBNJ) [1], [2]. By transmitting every symbol using multiple hops, FFH systems benefit from both time and frequency diversity, which assists in mitigating the detrimental effects of PBNJ. Furthermore, in the FFH-MFSK receiver, a suitable diversity-combining method may be invoked to further suppress the effects of PBNJ [1].

Although soft-decision decoding (SDD) of noncoherent MFSK-based schemes, including slow frequency hopping (SFH), have been investigated in the published literature [3]–[8], SDD-assisted FFH schemes have attracted little attention. The reasons for this trend might be the difficulty to derive soft information from the received signal, as well as the challenge of the subsequent exploitation of the soft information forwarded by the soft-input–soft-output (SISO) decoder to the demodulator. By contrast, a number of useful tools have been employed for the analysis, as well as for the performance enhancement, of iteratively decoded coherently modulated schemes [9]–[11]. A powerful technique to improve the iterative gain of iteratively decoded schemes is constituted by precoders, which improves the extrinsic information exchange between the channel decoder and the demodulator [11]. The precoder imposes memory upon the channel, thus rendering it recursive.[1] Hence, SISO systems have been shown to substantially benefit from employment of rate-1 precoders without reducing the effective throughput of the system [11].

In analogy to irregular convolutional codes (IrCCs) [9], the novel family of so-called irregular variable-length codes (IrVLCs) [12] employs a number of component variable-length coding (VLC) codebooks having different coding rates [13], [14] to encode particular fractions of the input source symbol stream. With the aid of EXtrinsic Information Transfer (EXIT) charts [10], the appropriate lengths of these fractions may be chosen to shape the inverted EXIT curve of the IrVLC codec to ensure that it does not cross the EXIT curve of the inner channel codec. This way, an open EXIT chart tunnel may be created, even at low signal-to-noise ratio (SNR) values. In [15], we proposed serial concatenation of an FFH-MFSK demodulator, a rate-1 decoder, and an IrVLC decoder and investigated the two-stage mutual information (MI) exchange between the rate-1 decoder and an IrVLC decoder. In this paper, we extend this concept to the three-stage extrinsic information exchange among the demodulator, the inner decoder, and the outer decoder. By employing EXIT charts, we investigate the serial concatenation of the FFH-MFSK demodulator, the rate-1 decoder, and the IrVLC outer decoder to attain good performance, even at low SNR values. We contrast the two-stage iterative decoding (ID) scheme between the inner rate-1 decoder and the IrVLC outer decoder to the three-stage scheme and demonstrate that the three-stage scheme outperforms the two-stage scheme. The proposed system might find fruitful application in FFH-MFSK-based ad hoc or cellular networks transmitting, for example, VLC-compressed H.264/MPEG4 video or audio signals. VLC compression may also provide useful data rate and bandwidth efficiency gains in pure data transmission by exploiting the potential latent correlation of bits.

II. SYSTEM OVERVIEW

In this section, we consider an IrVLC codec and an equivalent regular VLC-based benchmarker in this role. We refer to these schemes as the IrVLC- and VLC-FFH-MFSK arrangements, respectively. The schematic that is common to both of these schemes is shown in Fig. 1. We consider $K = 16$-ary source symbol values that have the probabilities of occurrence that result from the Lloyd–Max (LM) quantization [15], [16] of independent Laplacian distributed source samples. In the transmitter of Fig. 1, the source symbol frame $\mathbf{s}$ to be transmitted is partitioned into J 4-bit source symbols corresponding to $K = 16$-ary values of $\{s_j\}_{j=1}^J \in [1, \ldots, K]$. These 4-bit source symbols are then decomposed into N component streams $\{\mathbf{s_n}\}_{n=1}^N$ to be protected by N different rate IrVLC component codes, where we opted for $N = 16$ in the case of the IrVLC-FFH-MFSK scheme and $N = 1$ in the case of the VLC-based benchmarker scheme. The number of symbols in the source symbol frame $\mathbf{s}$ that are decomposed into the source symbol frame component $\mathbf{s_n}$ is specified as J_n, where we have $J_1 = J$ in the case of the VLC-based scheme. By contrast, in the case of the IrVLC-based scheme, the specific values of $\{J_n\}_{n=1}^N$ may be chosen to shape the inverted EXIT curve of the IrVLC codec

The authors are with the School of Electronics and Computer Science, University of Southampton, Southampton SO17 1BJ, U.K. (e-mail: sa03r@ecs.soton.ac.uk; rm02r@ecs.soton.ac.uk; lly@ecs.soton.ac.uk; lh@ecs.soton.ac.uk).

[1]Recursivity in this context implies that the channel has an infinite impulse response (IIR).
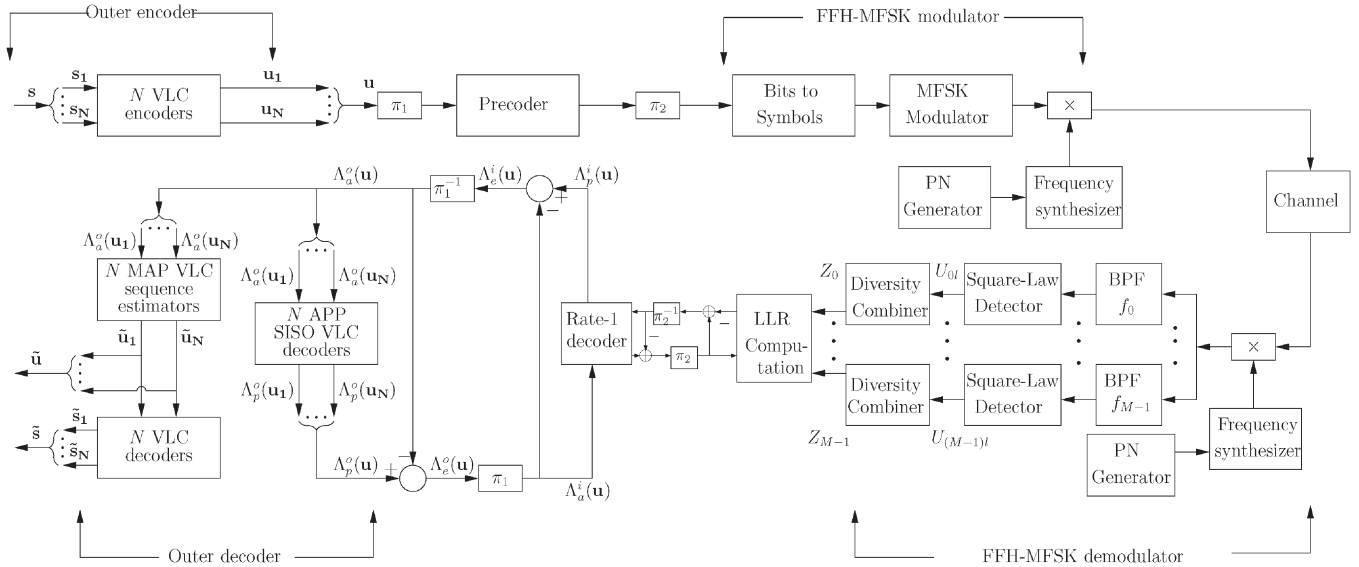
Fig. 1. Schematic of the IrVLC- and VLC-based schemes, employing three-stage serial concatenation of the demodulator, the rate-1 decoder, and the outer VLC/IrVLC decoder. In the IrVLC-coded scheme, $N = 16$, whereas in the VLC-coded scheme, $N = 1$.

so that it does not cross the EXIT curve of the precoder, as detailed in Section IV.[2]

Each of the N source symbol frame components $\{\mathbf{s_n}\}_{n=1}^N$ is VLC encoded using the corresponding codebook from the set of N VLC codebooks $\{\mathbf{VLC}_n\}_{n=1}^N$, having a range of coding rates $\{R_n\}_{n=1}^N \in [0, 1]$, satisfying $\sum_{n=1}^N \alpha_n R_n = R$, where $\alpha_n = J_n/J$ is the particular fraction of the source symbol frame coded by the nth subcode, and R is the average code rate of the VLC or the IrVLC scheme. The N VLC codewords that represent the J_n source symbols in the source symbol frame component $\mathbf{s_n}$ are concatenated to provide the transmission frame component $\mathbf{u_n}$. Owing to the variable length of the VLC codewords, the number of bits comprised by each transmission frame component $\mathbf{u_n}$ will typically vary from frame to frame. To facilitate VLC decoding of each transmission frame component $\mathbf{u_n}$, it is necessary to explicitly convey the exact number of bits I_n to the receiver with the aid of side information. This may be achieved using a low-rate block code or repetition code, for example. For the sake of avoiding obfuscating details, this is not explicitly shown in Fig. 1.

The N transmission frame components $\{\mathbf{u_n}\}_{n=1}^N$ encoded by the different IrVLC component codes are concatenated at the transmitter, as shown in Fig. 1. The resultant transmission frame $\mathbf{u}$ has a length of $\sum_{n=1}^N I_n$ bits. Following the bit interleaver, the binary transmission frame $\mathbf{u}$ is precoded, and the precoded bits are converted to M-ary symbols [7], which are transmitted by the FFH-MFSK modulator of Fig. 1. To further elaborate, in the FFH-MFSK transmitter, the M-ary symbols are mapped to M frequency tones [17]. The particular MFSK tone chosen for transmission modulates a carrier generated by a frequency synthesizer, which is controlled by the L-tuple FFH address

generated by a pseudonoise (PN) generator, where L is the number of frequency hops per symbol. T_s by $T_h = T_s/L$.

The channel is assumed to be a frequency-flat Rayleigh fading medium for each of the transmitted frequencies. Furthermore, we assume that the separation between the adjacent frequencies is $R_h = 1/T_h$, which also represents the bandwidth occupied by a single FFH-MFSK tone and is higher than the coherence bandwidth of the channel. Therefore, all FFH tones conveying the same symbol experience independent fading. The transmitted signal is also corrupted by additive white Gaussian noise and a PBNJ signal [17] having single-sided power spectral densities of N_0 and N_J, respectively. We assume that the PBNJ signal jams a fraction $0 \le \rho \le 1$ of the total spread-spectrum bandwidth W_{ss}, as discussed in [15].

The receiver schematic is also shown in Fig. 1, where the frequency dehopper, which is identical to and aligned with the frequency hopper of the transmitter, despreads the received signal using the knowledge of the transmitter's unique FFH address. The demodulator is composed of M branches, each corresponding to a single MFSK tone and consisting of a square-law detector [17] and a diversity combiner, which performs clipping followed by linear combining of the signals received in all hops. The process of clipping may be expressed by [1]

$$f(U_{ml}) = \begin{cases} C, & \text{if } U_{ml} \ge C \\ U_{ml}, & \text{otherwise} \end{cases}$$
$$m = 0, 1, \dots, M-1; \quad l = 0, 1, \dots, L-1 \qquad (1)$$

where U_{ml} represents the square-law detector's output corresponding to the mth tone in the lth hop, and C represents an appropriately chosen clipping threshold. The decision variable recorded after clipped combining is given by $Z_m = \sum_{l=0}^{L-1} f(U_{ml})$, $m = 0, 1, \dots, M-1$. Using the diversity combiner outputs, the corresponding symbol probabilities and log-likelihood ratios (LLRs) are computed, as explained in the following section, which are then fed to the rate-1 decoder.

---

[2]In this context, the authors would like to gratefully acknowledge the helpful comment of the anonymous reviewer that by designing the IrVLC code for the sake of approaching the capacity, it may seem that we have to surrender some of the flexibility in designing the VLC code to match the source statistics, which would potentially reduce the achievable compression ratio. We note, however, that this potential problem was circumvented by our two-stage design, where in the first stage, we designed the VLC codebook for $K = 16$-ary source symbol values generated from LM quantized independent Laplacian distributed source samples. In the second stage, the resultant stream of 4-bit symbols was then decomposed into N substreams encoded by the N IrVLC component codes. The IrVLC source-code design is, hence, decoupled from the near-capacity EXIT-chart matching.

III. ITERATIVE DECODING

In this section, we discuss how soft information is derived from the channel's output observations and how ID is carried out by exchanging extrinsic information between the demodulator, the rate-1 decoder, and the outer decoder, as shown in Fig. 1.

To compute the LLRs, we need the probability that the mth symbol or FSK tone was transmitted, $m = 0, \ldots, M - 1$, given that $\mathbf{Z} = [Z_0, Z_1, \ldots, Z_{M-1}]$ is received, which represents the set of M outputs of the diversity combiners of Fig. 1. This probability is given by

$$P(m|\mathbf{Z}) = \frac{p(\mathbf{Z}|m)P(m)}{p(\mathbf{Z})} \qquad (2)$$

where $p(\mathbf{Z}|m)$ is the probability density function (pdf) of the received signal $\mathbf{Z}$, given that the mth symbol is transmitted. Furthermore, $P(m)$ is the *a priori* probability of the symbol m, whereas $p(\mathbf{Z}) = \sum_{m=0}^{M-1} p(\mathbf{Z}|m)P(m)$ is the pdf of the received signal set $\mathbf{Z}$, which is the same for all m. Moreover, for equiprobable symbols, we have $P(m) = 1/M$. Hence, the pdf $p(\mathbf{Z}|m)$ uniquely and unambiguously describes the statistics required for estimating the probability $P(m|\mathbf{Z})$. For independent fading of all tones, the pdf $p(\mathbf{Z}|m)$ is given by

$$p(\mathbf{Z}|m) = f_{Z_m}(x_m|m) \prod_{n=0, \, n \neq m}^{M-1} f_{Z_n}(x_n|m) \qquad (3)$$

where $f_{Z_n}(x_n|m)$ represents the pdf of the nth diversity combiner output, $n = 0, 1, \ldots, M - 1$, given that the mth symbol is transmitted. To derive the pdfs of the diversity combiner outputs, we first consider the pdfs of the square-law detector outputs before diversity combining, as shown in Fig. 1. Assuming that the mth symbol is transmitted in the lth hop, it can readily be shown that for independent Rayleigh fading, the pdf of the square-law detector output U_{ml}, as shown in Fig. 1, may be expressed as [15], [17]

$$f_{U_{ml}}(y_m|m) = \frac{1}{1 + \gamma_h} e^{\frac{-y_m}{1+\gamma_h}}, \qquad y_m \geq 0 \qquad (4)$$

where $\gamma_h = bRE_b/(N_0 L)$ is the SNR per hop, E_b is the transmitted energy per bit, and $b = \log_2 M$ is the number of bits per symbol. From (4), using the characteristic function (CF) approach [17],[3] we can derive the pdf of the linear combiner's output Z_m, as shown in Fig. 1, which can be expressed as

$$f_{Z_m}(x_m|m) = \frac{x_m^{L-1}}{(1 + \gamma_h)^L \Gamma(L)} e^{-x_m/(1+\gamma_h)}. \qquad (5)$$

Similarly, for all the nonsignal tones, $n = 0, 1, \ldots, M - 1, n \neq m$, we have

$$f_{Z_n}(x_n|m) = \frac{x_n^{L-1}}{\Gamma(L)} e^{-x_n}. \qquad (6)$$

Inserting (5) and (6) in (3) and after further simplifications, we have

$$p(\mathbf{Z}|m) = \left[\frac{1}{(1+\gamma_h)^L} \frac{1}{\Gamma^M(L)} \prod_{n=0}^{M-1} x_n^{L-1} e^{-x_n} \right] \exp\left(\frac{x_m \gamma_h}{1+\gamma_h} \right). \qquad (7)$$

We can see in (7) that all the terms except the last exponential term are common for any of the mth symbol, $m = 0, 1, \ldots, M - 1$. Since the computation of the LLRs requires the logarithm of the bit probabilities, we consider the common terms as a normalization factor and express the normalized probability $p(\mathbf{Z}|m)$ as

$$p(\mathbf{Z}|m) = \exp\left(\frac{x_m \gamma_h}{1+\gamma_h} \right). \qquad (8)$$

---

[3]The CF is the Fourier transform of the pdf, and the fact that the CF of a sum of random variables is the product of their individual CFs [17] has been exploited here.
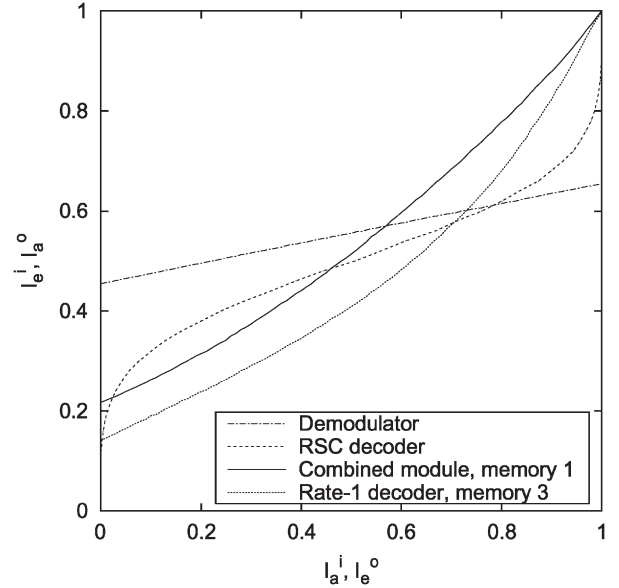

Fig. 2. EXIT characteristics of the demodulator, the rate-1 decoder, and the combined module in Rayleigh fading channels contaminated by PBNJ, assuming $E_b/N_0 = 6$ dB, $E_b/N_J = 10$ dB, and $\rho = 0.1$.

Upon inserting (8) in (2), we can derive the corresponding symbol probabilities. The resultant bit probabilities can be derived from the symbol probabilities, assuming the bits-to-symbol mapping of [7]. Finally, the LLRs can be computed using the bit probabilities [10]. Note that earlier in this paper, we have derived the soft information from the channel's output observations, assuming a somewhat simplistic but tractable interference-free channel. Moreover, although clipped combining is employed, our analysis assumes linear combining, i.e., without clipping. This assumption has been stipulated for the sake of further simplifying the analysis and is supported by the observation that clipping is an operation performed to reduce effects of PBNJ. We will demonstrate in Section IV that valuable performance improvements can be achieved using this suboptimal soft information.

Following the derivation of the soft information from the received signal, two types of serial concatenation schemes are possible. In the first case, the *a posteriori* probability (APP) SISO rate-1 decoder and the outer decoder perform ID [15], [18]. We refer to this configuration of the ID as the *two-stage scheme*. Alternatively, the system may be modified so that the FFH-MFSK demodulator, the rate-1 inner decoder, and the IrVLC outer decoder exchange their extrinsic MI, as shown in Fig. 1. We refer to this arrangement as the *three-stage scheme*, which requires an additional interleaver between the precoder and the FFH-MFSK modulator of Fig. 1.

In [15], we demonstrated that the FFH-MFSK demodulator yields low-gradient EXIT curves for all values of the modulation order M. When the SNR is sufficiently high, the EXIT curves can be shifted upward in the EXIT plane, and hence, an arbitrarily low bit error ratio (BER) may be achieved. However, this would be achieved at the cost of having a large area between the demodulator's and the decoder's EXIT curves, implying that the scheme operates far from capacity. By contrast, it was shown in [15] that the precoder renders the channel to appear recursive [11], i.e., of IIR, and hence results in steeper EXIT curves than the stand-alone demodulator. Furthermore, as the precoder's memory is increased, the EXIT curves become steeper. Moreover, in contrast to the demodulator, the rate-1 decoder's EXIT curves do indeed reach the $(I_e, I_a) = (1, 1)$ point, implying that the precoder allows the ID to converge to an arbitrarily low BER.
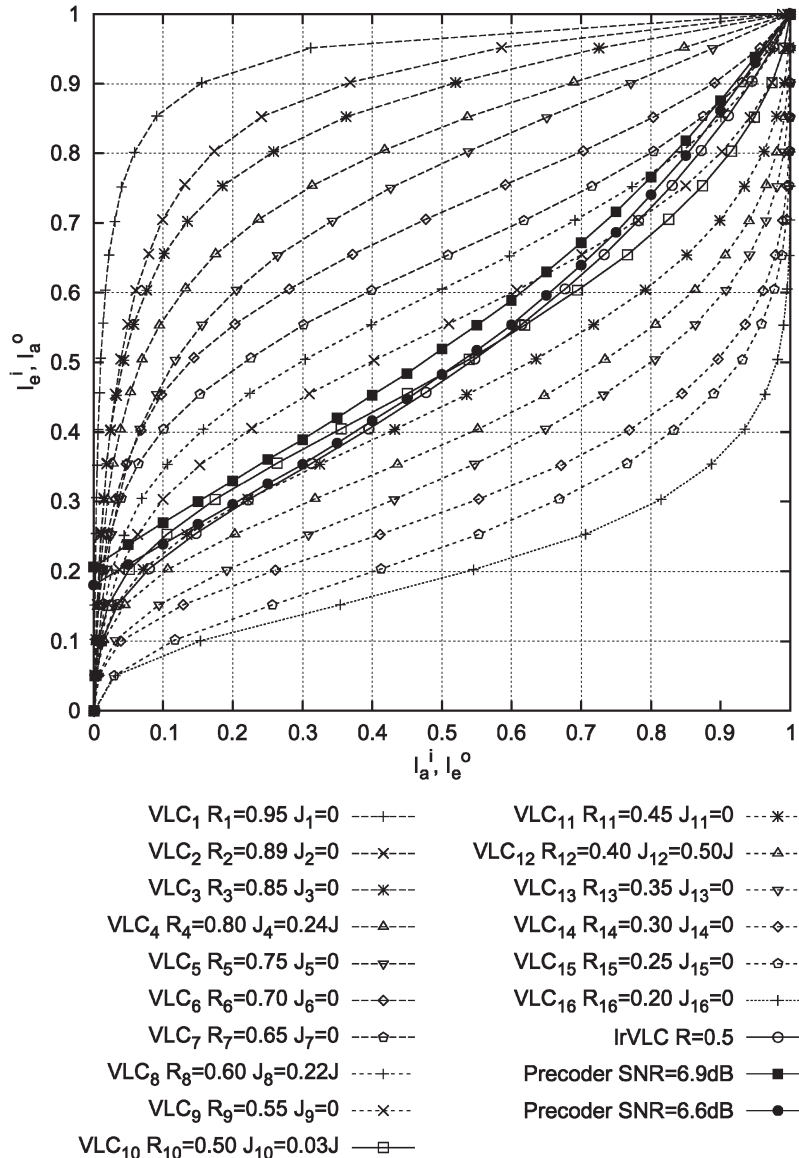
Fig. 3.   Inverted VLC EXIT curves and rate-1 decoder EXIT curves in uncorrelated Rayleigh fading channels, assuming $E_b/N_J = 10$ dB and $\rho = 0.1$.

Let us now employ the EXIT chart technique to investigate the three-stage receiver scheme, namely, the FFH-MFSK demodulator, the inner rate-1 decoder, and the outer IrVLC decoder. Ideally, this would require a 3-D EXIT chart depicting the evolution of the MI at the output of the three concatenated components. However, a simpler and almost equally effective method of investigating this three-way MI exchange was proposed in [19], which implies treating the FFH-MFSK demodulator and the rate-1 inner decoder as a single module, although they also exchange extrinsic information in a single step. This effectively allows us to analyze the three-stage concatenation as a two-stage one using 2-D EXIT charts. We will refer to this module as the *combined module*. All MI measurements were made using the histogram-based approximation of the true distribution [10]. Note that in Fig. 1, $\Lambda(\cdot)$ denotes the LLRs of the bits concerned, where the superscript i indicates the inner decoder (or demodulator), whereas o corresponds to the outer decoder. Additionally, a subscript denotes the dedicated role of the LLRs, with a, p, and e indicating *a priori*, *a posteriori*, and extrinsic information, respectively. More-over, unless otherwise stated, we employ the following parameter values: source symbol frame length $J = 70\,000$, code rate $R = 0.5$,

MFSK modulation order of $M = 16$, and FFH diversity order of $L = 3$. Finally, we assume having the optimum clipping thresholds defined in (1) for all simulations [1]. Usually, the most suitable clipping levels for various values of the system parameters can be determined in an empirical manner, e.g., by plotting the system BER against the clipping level and choosing the clipping threshold that yields the lowest BER.

In Fig. 2, we compare the EXIT characteristics of the three types of inner modules considered, when the channel was also contaminated by PBNJ. The inverted EXIT curve of a half-rate recursive systematic convolutional decoder characterized by the octal generator polynomial of (7,5) is also shown. We observe that the combined module has a su-perior EXIT curve, and although its EXIT curve has a similar gradient as that of the rate-1 decoder, its EXIT curve emerges from a higher point in the EXIT plane at a zero abscissa value, indicating that the combined module would allow satisfactory communication at lower SNR values. The superiority of the combined module over the stand-alone rate-1 decoder stems from the fact that when employing the combined module, MI is exchanged between the two SISO modules, i.e., the demodulator and the rate-1 decoder, thus enabling optimum exploitation of the soft information.
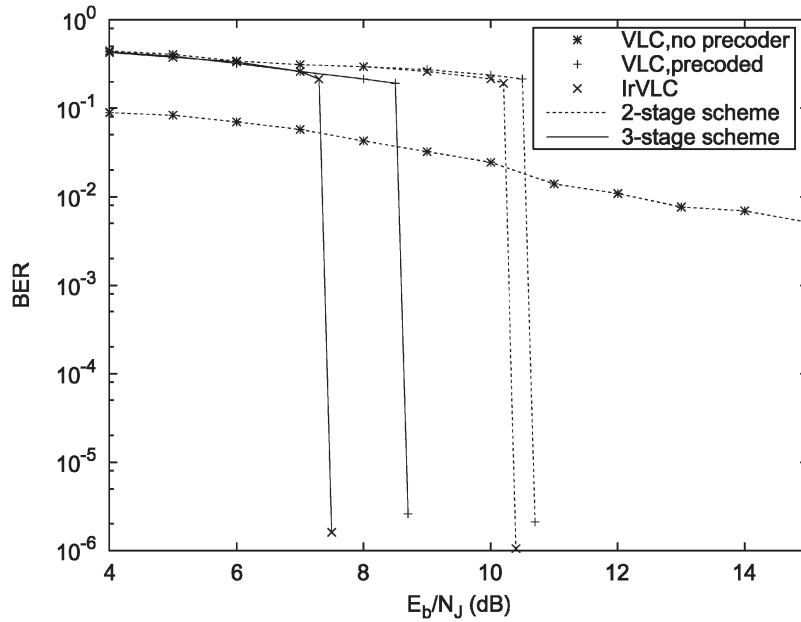
Fig. 4.   BER versus E_b/N_J performance of the two- and three-stage VLC- and IrVLC-based schemes in jammed uncorrelated Rayleigh fading channels, assuming $E_b/N_0 = 10$ dB and $\rho = 0.5$.

Note that our combined module invokes a single iteration of MI exchange between the demodulator and the rate-1 decoder. We have also investigated the use of more than one iterations between these two blocks, but it was found that virtually no additional benefits were achieved to justify its added complexity. Hence, when the three-stage scheme of Fig. 1 is employed, each ID iteration involves one iteration between the demodulator and the rate-1 decoder, followed by a single iteration between the rate-1 inner decoder and the outer decoder. Moreover, for the three-stage scheme, we invoke a precoder of memory 1, whereas for the two-stage scheme, we employ a precoder of memory 3, since using these precoder memories, attractive EXIT characteristics are achieved.

Since N separate VLC encoders are employed in the IrVLC-FFH-MFSK transmitter, N separate VLC decoders are employed in the corresponding receiver seen in Fig. 1. The *a priori* LLRs $\Lambda_a^o(\mathbf{u})$ are decomposed into N components, as shown in Fig. 1. This is achieved with the aid of the explicit side information that we assume for conveying the number of bits I_n in each transmission frame component $\mathbf{u_n}$. Each of the N VLC decoders is provided with the *a priori* LLR subframe $\Lambda_a^o(\mathbf{u_n})$, and in response, it generates the *a posteriori* LLR subframe $\Lambda_p^o(\mathbf{u_n})$, $n \in [1, \ldots, N]$. These *a posteriori* LLR subframes are concatenated to provide the *a posteriori* LLR frame $\Lambda_p^o(\mathbf{u})$, as shown in Fig. 1. During the final decoding iteration, N bit-based MAP VLC sequence estimation processes are invoked instead of single-class APP SISO VLC decoding, as shown in Fig. 1. In this case, each transmission frame component $\mathbf{u_n}$ is estimated from the corresponding *a priori* LLR frame component $\Lambda_a^o(\mathbf{u_n})$. The resultant transmission frame component estimates $\tilde{\mathbf{u}}_\mathbf{n}$ of Fig. 1 may be concatenated to provide the transmission frame estimate $\tilde{\mathbf{u}}$, as explained in [15].

IV. SYSTEM PARAMETER DESIGN AND RESULTS

In Fig. 3, we provide the inverted EXIT curves that characterize the bit-based APP SISO VLC decoding of the aforementioned VLC codebooks, together with the rate-1 decoder's EXIT curves at E_b/N_0 values of 6.6 and 6.9 dB. All the EXIT curves were generated using uncorrelated Gaussian distributed *a priori* LLRs, based on the assumption that the transmission frame's bits have equiprobable logical values

[15]. Fig. 3 also shows the inverted EXIT curve of the IrVLC scheme. This was obtained as the appropriately weighted superposition of the $N = 16$ component VLC codebooks' inverted EXIT curves, where the weight applied to the inverted EXIT curve of the component VLC codebook $\mathbf{VLC_n}$ is proportional to the specific number of source symbols employed for encoding J_n [9]. Using the approach of [9], the values of $\{J_n\}_{n=1}^N$ given in Fig. 3 were designed so that the IrVLC coding rate matches that of our regular VLC scheme, namely, 0.5. Furthermore, we ensured that the inverted IrVLC EXIT curve did not cross the rate-1 decoder's EXIT curve at $E_b/N_0 = 6.6$ dB. As shown in Fig. 3, the presence of the resultant open EXIT chart tunnel implies that an infinitesimally low BER may be achieved by the IrVLC-FFH-MFSK scheme for E_b/N_0 values above 6.6 dB. By contrast, having an open EXIT chart tunnel is not afforded for E_b/N_0 values below 6.9 dB in the case of the benchmarker VLC-based scheme, which is identical to the VLC codebook $\mathbf{VLC}_{10}$ of the IrVLC scheme. Analogous to the IrVLC design of Fig. 3, we have designed IrVLC codes for both the two- and three-stage ID schemes, assuming various jamming scenarios in Rayleigh fading channels.

Let us now focus our attention on the BER performance of the proposed system in the context of the two- and three-stage schemes considered. Note that the BER depicted in Figs. 4 and 5 corresponds to the encoded bits of the transmission frame $\mathbf{u}$ and the corresponding received frame $\tilde{\mathbf{u}}$.

In Fig. 4, we provide the BER versus E_b/N_J performance comparison of the two- and three-stage schemes, assuming $E_b/N_0 = 10$ dB and $\rho = 0.5$. We observe that both the VLC- and IrVLC-based schemes result in superior performance compared to the system operating without the precoder, which encounters an error floor. We also note that the three-stage IrVLC scheme yields a further improvement of nearly 3 dB over the two-stage IrVLC scheme. This performance gain confirms the EXIT chart prediction of Fig. 2. Finally, we note in Fig. 4 that the IrVLC-based three-stage scheme outperforms the corresponding VLC-based scheme by approximately 1.1 dB.

An increased complexity is imposed by the increased number of decoding iterations, which is a natural consequence of operating at lower SNRs. This is particularly true in the case of the IrVLC scheme, where typically a narrower EXIT tunnel exists between the EXIT
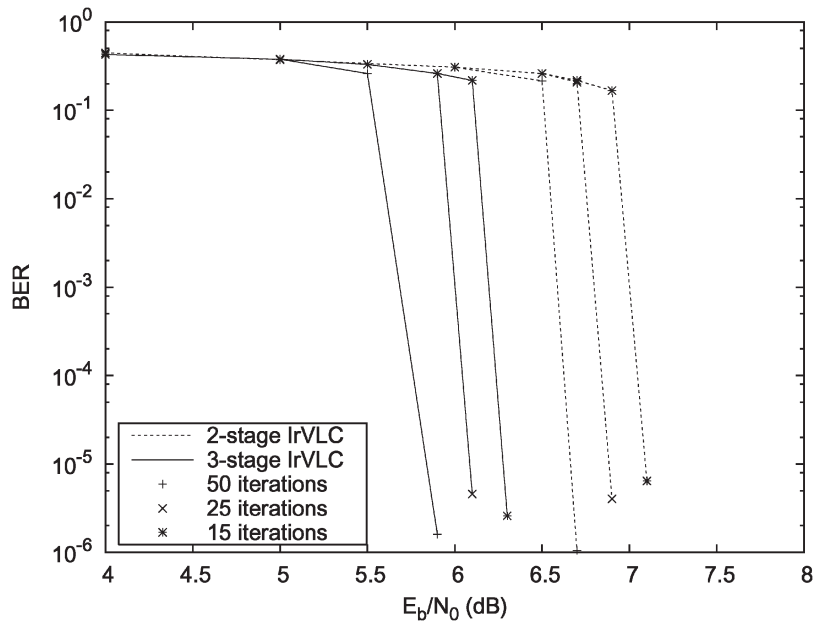
Fig. 5.   BER versus E_b/N_0 performance of the two- and three-stage IrVLC-based schemes in jammed uncorrelated Rayleigh fading channels for various numbers of decoding iterations, assuming $E_b/N_J = 10$ dB and $\rho = 0.1$.

curves of the outer and inner decoders, as shown in Fig. 3. In Fig. 4, up to 80 iterations are needed for achieving convergence to the point of $(I_e, I_a) = (1, 1)$, which is associated with an infinitesimally low BER, when employing the proposed IrVLC-based scheme. The effect of reducing the number of iterations on both the two- and three-stage schemes is depicted in Fig. 5, where the BER versus E_b/N_0 performance of the IrVLC schemes considered is shown. We observe that the number of decoding iterations can significantly be reduced by increasing the E_b/N_0 value by as little as 0.2–0.4 dB.

V. CONCLUSION

We have investigated the serial concatenation of IrVLC coding with an FFH-MFSK modem operating in a Rayleigh fading channel when the transmitted signal was corrupted by PBNJ. We employed 2-D EXIT charts to investigate the three-stage concatenation of the FFH-MFSK demodulator, the rate-1 decoder, and the outer IrVLC decoder. Furthermore, the IrVLC code was designed in such a way that the inverted EXIT curve of the IrVLC decoder matches the EXIT curve of the inner decoder. This way, an open EXIT chart tunnel may be created, even at low SNR values, providing source-correlation-dependent additional performance gains of up to 1.1 dB over the VLC-based scheme. Consequently, we noted that the precoder-aided schemes yield E_b/N_0 gains in excess of 7 dB over the system dispensing with the precoder, which suffers from an error floor, when jamming is severe. Moreover, we demonstrated that the three-stage concatenated scheme yields approximately 3-dB better performance compared with the two-stage arrangement.

REFERENCES

[1] K. C. Teh, A. C. Kot, and K. H. Li, "FFT-based clipper receiver for fast frequency-hopping spread-spectrum system," in *Proc. IEEE Symp. Circuits Syst.*, May/Jun. 1998, vol. 4, pp. 305–308.
[2] X. F. Wu, C. M. Zhao, X. H. You, and S. Q. Li, "Robust diversity-combing receivers for LDPC coded FFH-SS with partial-band interference," *IEEE Commun. Lett.*, vol. 11, no. 7, pp. 613–615, Jul. 2007.
[3] P. C. P. Liang and W. E. Stark, "Algorithm for joint decoding of turbo codes and M-ary orthogonal modulation," in *Proc. IEEE Int. Symp. Inf. Theory*, Jun. 2000, p. 191.
[4] K. Cheun and W. E. Stark, "Performance of robust metrics with convolutional coding and diversity in FHSS systems under partial-band noise jamming," *IEEE Trans. Commun.*, vol. 41, no. 1, pp. 200–209, Jan. 1993.
[5] M. C. Valenti and S. Cheng, "Iterative demodulation and decoding of turbo-coded M-ary noncoherent orthogonal modulation," *IEEE J. Sel. Areas Commun.*, vol. 23, no. 9, pp. 1739–1747, Sep. 2005.
[6] Q. Zhang and T. Le-Ngoc, "Turbo product codes for FH-SS with partial-band interference," *IEEE Trans. Wireless Commun.*, vol. 1, no. 3, pp. 513–520, Jul. 2002.
[7] U. C. Fiebig, "Soft-decision and erasure decoding in fast frequency-hopping systems with convolutional, turbo, and Reed–Solomon codes," *IEEE Trans. Commun.*, vol. 47, no. 11, pp. 1646–1654, Nov. 1999.
[8] D. Park and B. G. Lee, "Iterative decoding in convolutionally and turbo coded MFSK/FH-SSMA systems," in *Proc. IEEE ICC*, Jun. 2001, vol. 9, pp. 2784–2788.
[9] M. Tüchler and J. Hagenauer, "EXIT charts of irregular codes," in *Proc. Conf. Inf. Sci. Syst.*, Princeton, NJ, Mar. 2002, pp. 748–753.
[10] S. ten Brink, "Convergence of iterative decoding," *IEEE Trans. Commun.*, vol. 49, no. 10, pp. 1727–1737, Oct. 2001.
[11] R. Y. S. Tee, S. X. Ng, and L. Hanzo, "Precoder-aided iterative detection assisted multilevel coding and three-dimensional EXIT-chart analysis," in *Proc. IEEE WCNC*, Apr. 2006, vol. 3, pp. 1322–1326.
[12] R. G. Maunder, J. Wang, S. X. Ng, L.-L. Yang, and L. Hanzo, "Iteratively decoded irregular variable length coding and trellis coded modulation," in *Proc. IEEE Workshop Signal Process. Syst.*, Shanghai, China, Oct. 2007, pp. 222–227.
[13] V. Buttigieg and P. G. Farrell, "Variable-length error-correcting codes," *Proc. Inst. Elect. Eng.—Commun.*, vol. 147, no. 4, pp. 211–215, Aug. 2000.
[14] R. Bauer and J. Hagenauer, "Iterative source/channel-decoding using reversible variable length codes," in *Proc. Data Compression Conf.*, Snowbird, UT, 2000, pp. 93–102.
[15] S. Ahmed, R. G. Maunder, L. L. Yang, S. X. Ng, and L. Hanzo, "Joint source coding, unity rate precoding and FFH-MFSK modulation using iteratively decoded irregular variable length coding," in *Proc. 66th IEEE VTC—Fall*, Sep./Oct. 2007, pp. 1042–1046.
[16] S. Lloyd, "Least squares quantization in PCM," *IEEE Trans. Inf. Theory*, vol. IT-28, no. 2, pp. 129–137, Mar. 1982.
[17] J. G. Proakis, *Digital Communications*.   Singapore: McGraw-Hill, 2001.
[18] V. B. Balakirsky, "Joint source-channel coding with variable length codes," in *Proc. IEEE Int. Symp. Inf. Theory*, Ulm, Germany, Jun. 1997, p. 419.
[19] J. Wang, S. X. Ng, A. Wolfgang, L.-L. Yang, S. Chen, and L. Hanzo, "Near-capacity three-stage MMSE turbo equalization using irregular convolutional codes," in *Proc. Int. Symp. Turbo Codes*, Munich, Germany, Apr. 2006. Electronic publication.